



## Research article

## Thin poly(vinyl alcohol) cryogels: reactive groups, macropores and translucency in microtiter plate assays

Alexander E. Ivanov<sup>a</sup>, Lennart Ljunggren<sup>b,\*</sup><sup>a</sup> *VitroSorb AB, Medeon Science Park, Per Albin Hanssons Väg 41, SE-20512, Malmö, Sweden*<sup>b</sup> *Malmö University, Faculty of Health and Society, Department of Biomedical Science, SE-20506, Malmö, Sweden*

## ARTICLE INFO

## Keywords:

Chemistry  
Chemical engineering  
Materials science  
Multiwell  
Aldehyde  
Film  
Photometry  
Hydrogel

## ABSTRACT

Thin macroporous poly(vinyl alcohol) (PVA) hydrogels were produced by cross-linking of PVA in a semi-frozen state with glutaraldehyde (GA) on glass slides or in the wells of microtiter plates. The 100–130  $\mu\text{m}$ -thick gels were mechanically transferable, squamous translucent films with a high porosity of  $7.2 \pm 0.3 \text{ mL/g}$  dry PVA *i.e.* similar to larger cylindrical PVA monoliths of the same composition. Additional treatment of the gels with 1% GA increased the aldehyde group content from 0.7 to 2.4  $\mu\text{mol/mL}$  as estimated using dinitrophenylhydrazine (DNPH) reagent. Translucency of the gels allowed registration of UV-visible spectra of the DNPH-stained films. The catalytic activity of trypsin covalently immobilized on thin gels in the microtiter plates was estimated with chromogenic substrate directly in the wells, and indicated that the amount of protein immobilized was at least 0.34 mg/mL gel. Human immunoglobulin G (IgG) immobilized on thin gels at 0.1–10 mg/mL starting concentrations could be detected in a concentration-dependent manner due to recognition by anti-human rabbit IgG conjugated with peroxidase and photometric registration of the enzymatic activity. The results indicate good permeability of the hydrogel pores for macromolecular biospecific reagents and suggest applications of thin reactive PVA hydrogels in photometric analytical techniques.

## 1. Introduction

Cryogels are hydrogels produced by polymerization of water-soluble monomers or cross-linking of water-soluble polymers under semi-frozen states [1]. These spongy, macroporous and flow permeable materials have gained an increasing attention as separation media, cell culture substrates as well as medical and environmental adsorbents during the last two decades [2]. An attractive property of cryogels, which has rarely been studied, is their translucency allowing photometric studies. Recently, a radiochromic dosimeter [3] has been developed by incorporation of xylenol orange – iron (II) complexes into a poly(vinyl alcohol) (PVA) cryogel. Thin hydrogels of gelatin [4], polyacrylamide [5] or poly(N,N-dimethylacrylamide) [6] produced in non-frozen solutions were earlier studied as immobilization media for reactive dyes able to change their spectral characteristics in response to low molecular weight analytes such as metal ions or saccharides. Many examples of optically responsive hydrogels can be found in the reviews [7, 8].

It is pertinent to employ thin translucent cryogels in bioanalytical photometric techniques. Since typical internal structure of cryogels exhibits a pattern of interconnected macropores with diameters up to 100

or 200  $\mu\text{m}$ , their permeable network may facilitate immobilization and/or molecular recognition of high molecular weight analytes. The large pores accommodate not only biopolymers but also biological cells that can be visualized by immunofluorescent staining and confocal laser scanning microscopy [9, 10, 11]. Regarding manufacturing of thin, flat translucent cryogels, the question arises if these can be made as monolithic and mechanically transferable porous films, and the present work gives a positive answer. Our aim was to prepare thin cryogel films, characterization of their microscopic texture, porosity and functional group content, as well as their adaptation to microtiter plate measurements with optical detection. To the best of our knowledge, the above issues taken as a whole have not been addressed up to now.

Among the variety of cryogels employed for bioapplications, PVA gels have drawn much attention due to the ease of manufacture by means of chemical cross-linking of PVA by glutaraldehyde (GA) in semi-frozen aqueous medium [12, 13]. Typically, the reactive aldehyde functions of GA remaining after the cross-linking were coupled to ethanolamine [12], or were reduced using sodium borohydride [13] to provide gels with non-fouling characteristics. To perform immobilization of bioaffinity ligands (e.g. proteins), some authors preferred additional

\* Corresponding author.

E-mail address: [lennart.ljunggren@mau.se](mailto:lennart.ljunggren@mau.se) (L. Ljunggren).

activation of the matrix with another reagent, for example, epichlorohydrin [10], instead of further treatment by GA. The latter type of PVA activation was shown, however, to be effective for immobilization of staphylococcal protein A via its coupling to the surface-bound aldehydes [14]. Similar method for coupling of laccase to PVA cryogels activated by GA has been reported [15]. Previously, apart from macroscopic gels, many other aldehyde-containing supports, such as polymer microspheres [16] or chromatography matrices [17], were successfully used for immobilization of specific antibodies and other biomolecules. The scheme of PVA chemical cross-linking followed by further treatment of the gel with GA is given in Figure 1.

Lack of knowledge on the quantity of reactive aldehyde groups, their accessibility for coupling to proteins, and the protein immobilization capacity, are possible limiting factors for a wider use of GA-activated PVA cryogels. In the present study, we show that the aldehyde groups can be estimated using conventional assay with dinitrophenylhydrazine (DNPH), moreover, the direct spectrophotometry of flat 100  $\mu\text{m}$ -thick PVA cryogels stained with this reagent can be performed. In solution, DNPH reacts with aldehydes yielding hydrazones, which precipitate from acidic ethanolic media, and the assay has long been used for identification and estimation of aldehydes [18, 19]. Recent studies reported

estimation of aldehyde groups in insoluble powders [20], where the quantity of aldehydes was calculated from the depletion of DNPH from the solution. Colorimetric monitoring of aldehydes in solid beads has also been described [21], though their coloration was detected visually without being quantified. This study is not aimed at the development of particular sensing technique but tends to demonstrate the opportunities suggested by thin PVA cryogels. To the best of our knowledge, this is the first report on photometric measurements where a thin PVA cryogel layer acts as a translucent support in a microtiter plate format.

## 2. Experimental

### 2.1. Materials

Poly(vinyl alcohol) (PVA), Mowiol 18-88,  $M_w = 130000$  g/mol, saponification degree 88%, was a product of Clariant GmbH (Frankfurt, Germany). Glutaraldehyde solution (25%, for electron microscopy) (GA) and 2,4-dinitrophenylhydrazine (DNPH) were purchased from Merck (Darmstadt, Germany). N-benzoyl-DL-arginine 4-nitroanilide hydrochloride (BAPNA), trypsin from bovine pancreas and immunoglobulin G from human serum were products of Sigma-Aldrich. Rabbit anti-human

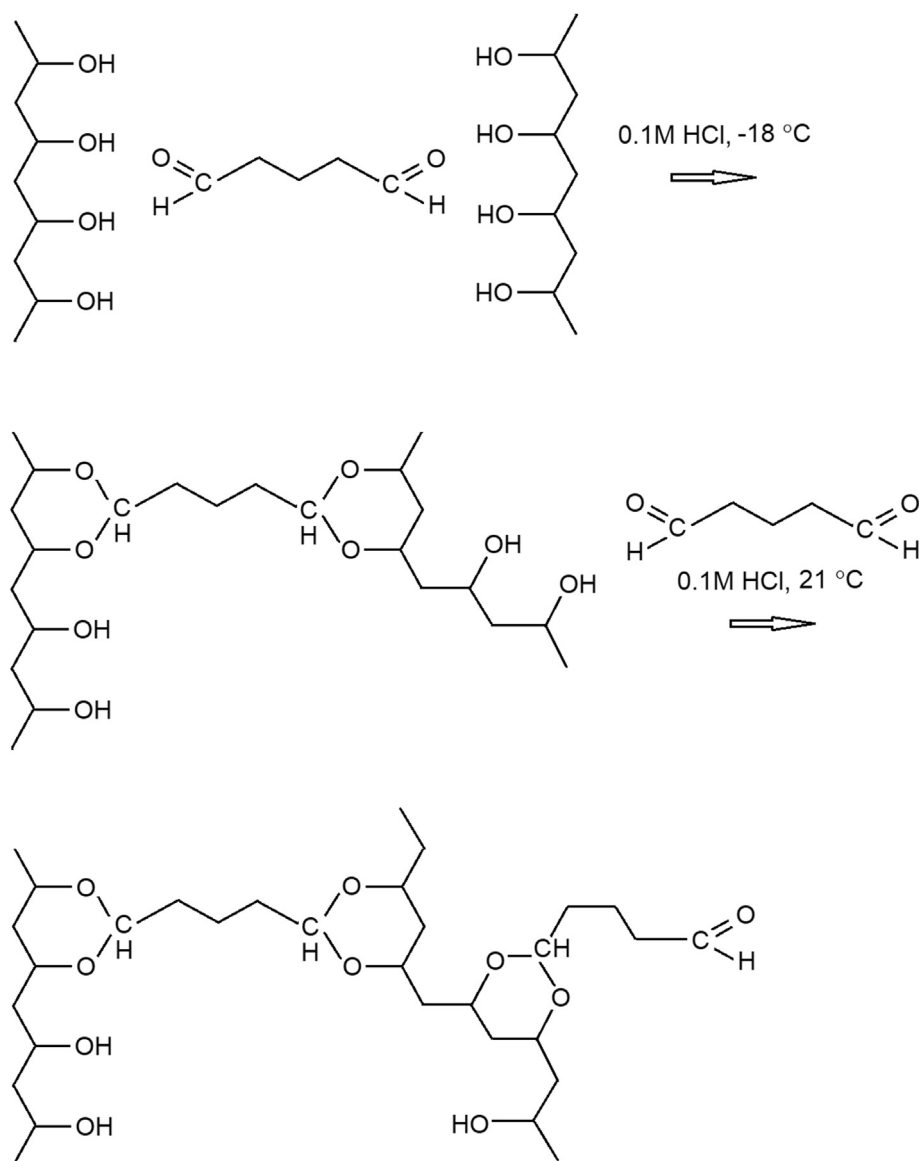


Figure 1. Scheme of PVA chemical cross-linking and further activation by GA.

IgG/HRP conjugate solution was a product of DAKO, Denmark. Dimethyl sulfoxide (DMSO) extra pure was from Scharlab S.L. (Sentmenat, Spain). Pellets used to make phosphate buffer saline (PBS) and PBS with 20 mM Tween were from Amresco, Solon, USA, and Medicago, Uppsala, Sweden, respectively. 3,3',5,5'-tetramethylbenzidine (TMB) Liquid Substrate, Super Slow for ELISA was from Sigma-Aldrich. Polystyrene Microtest Plates 96 Well F were from Sarstedt (Nümbrecht, Germany). Plastic Becton-Dickinson syringes (2 mL) were used as containers for synthesis of cryogels in shape of cylinders.

## 2.2. Synthesis and protein immobilization

### 2.2.1. Cryogel synthesis

Poly(vinyl alcohol) (PVA) cryogels were prepared following the previously described methods [12, 22]. Briefly, 5% w/v PVA solution in water (3.8 mL) was combined with 0.2 mL 2M HCl and cooled down to 0 °C in an ice bath. Aqueous glutaraldehyde (25%, 80 µL) was added to the polymer solution and the reaction mixture (50 µL) was applied to and spread on the surface of glass slides (9.5 × 40 mm), which were then horizontally placed in a freezer at -18 °C. To prepare cylindrical cryogels or cryogels in the wells of 96-well plates, the above mixture was added to plastic syringes or to wells, and cooled in a freezer down to -18 °C in air. The cross-linking reaction was allowed to proceed overnight, the cryogels were defrosted and rinsed by flow through of deionized water until zero absorbance ( $\lambda = 280$  nm) of the washings. For further chemical activation with glutaraldehyde (GA), the cryogels were brought into contact with 1%, 2.5% or 10% GA in 0.1 M HCl; kept at room temperature (21 °C) on a minirotator for 2 h and rinsed as above. For reduction of aldehyde groups, the cryogels were treated with cold, freshly made 50 mM sodium borohydride solution, 3–4 times with fresh volumes, kept in the same solution for 3 h at 4 °C and rinsed by water. The gels made on glass slides were 100–130 µm-thick films as calculated from their dimensions and wet weights.

### 2.2.2. Cryogel films made in a 96-well plate: immobilization of trypsin

To ensure adhesion of the cryogels to the plate wells, these were first filled by 20 µL 2.5% w/v PVA solution in 50% aqueous acetone, which evaporated under gentle heating on an electric plate, forming a thin transparent PVA coating; PVA is known to adhere well to polystyrene [23]. Then 40 µL of the PVA-GA reaction mixture made as described in Section 2.2.1 was added to the wells, frozen at -18 °C and kept overnight. After defrosting in contact with deionized water, the spongy gels were rinsed by suction/injection of water using a 1 mL-plastic dropper. Good physical adhesion of gels to the PVA-precoated plate allowed shaking of the plates without detachment. The wells were filled with 1% GA in 0.1 M HCl for chemical activation of the gels at room temperature for 2h. The thus activated gels were rinsed with water as described above, and then by 1M NaHCO<sub>3</sub>, pH 8.4, to reach this pH value in the gel pores. To remove excessive liquid, the plate was shaken and the gels slightly compressed by dry cotton wool sticks. The gels were combined either with 150 µL of 10 mg/mL trypsin solution in 1M NaHCO<sub>3</sub> (4 gels) or with water to get reference gel samples (4 gels). After keeping the gels at room temperature for 2 h, these were washed 10–12 times by deionized water using a plastic dropper until no enzyme activity could be found in the supernatants. The gels were then kept under cold 50 mM NaBH<sub>4</sub> in a fridge for 3 h and washed by deionized water to neutral pH.

### 2.2.3. Cryogel films made in a 96-well plate: immobilization of human immunoglobulin G (IgG) and its detection with anti-human peroxidase conjugated rabbit IgG

Immobilization of IgG was done similar to that of trypsin, using 1 M NaHCO<sub>3</sub> as a coupling solution, see Section 2.2.2, where IgG was dissolved at concentrations of 0.1, 1 and 10 mg/mL. Each of the solutions was added to four thin cryogels attached to the wells of a 96-well plate and kept at room temperature for 2h. The gels were washed by deionized water, treated by freshly made cold 50 mM NaBH<sub>4</sub> at 4 °C for 3h to

reduce the non-reacted aldehyde groups, and thoroughly (10–12 times) washed by phosphate buffered saline, pH 7.4 (PBS) containing 20 mM Tween, using a plastic dropper. Anti-human peroxidase conjugated rabbit IgG solution was diluted by the above buffer solution 5000 times, added (200 µL) to the wells with immobilized  $\gamma$ -globulin and allowed to bind to the protein for 1h. The gels were washed several times by the same buffer solution using a plastic dropper, then by 10% ethanol in 0.1M NaHCO<sub>3</sub> (pH 8.4), deionized water, 10 mM acetic acid (pH 3.4) and again with the buffer solution to neutral pH. TMB-ELISA substrate solution (100 µL) was added to the gels where human  $\gamma$ -globulin was immobilized as well as to the gels without  $\gamma$ -globulin. After 10 min the reaction was quenched with 0.3 M H<sub>2</sub>SO<sub>4</sub> and the absorbance of the colored product was read at 450 nm using a Power Wave XS ELISA reader (BIO-TEK Instruments, USA).

## 2.3. Physico-chemical characterization and analytical techniques

UV-VIS spectra of thin gels were recorded on a Shimadzu UV-1700 PharmaSpec spectrophotometer and processed using UV-Probr 2.31 software, Shimadzu Corporation. The spectrophotometer was also used for estimation of solute absorbances at particular wavelengths. Absorbances in the wells of microtiter plates were measured using a Power Wave XS ELISA reader (BIO-TEK Instruments, USA). An Olympus CX31 microscope equipped with an Infinity 3 Luminera digital CCD camera was used to take micrographs of wet cryogels made on the surface of glass slides. FTIR spectra were recorded on a Nicolet 6700 instrument with a Smart ITR accessory using 16 scans, a standard KBr beam splitter, the spectral range of 5000–400 cm<sup>-1</sup>, and resolution of 4 cm<sup>-1</sup>. All spectra were processed and analyzed using the OMNIC™ 8 Spectra Software. Cryogel sample preparation for FTIR-spectroscopy was the same as for electron microscopy, see Section 2.3.6.

### 2.3.1. Estimation of aldehyde groups in cylindrical cryogels

50 µM DNPH stock solution in 90% ethanol containing 2M H<sub>2</sub>SO<sub>4</sub> was made according to the method [20] and diluted 50-fold by 90% ethanol to obtain 1 mM DNPH, as needed for analyses. A cylindrical PVA cryogel (7 × 14 mm, V<sub>CR</sub> = 0.54 mL) was cut into ca. 2 mm-pieces and the pieces were added to 2 mL of 1 mM DNPH solution in 90% ethanol, containing 40 mM H<sub>2</sub>SO<sub>4</sub> and agitated by orbital rotation. Aliquots of the supernatant were taken from the reaction mixture at various times and centrifuged at 18800 rcf for 3 min. The centrifugate was further diluted 25 times and its absorbance at 360 nm (A<sub>360</sub>) was registered. The DNPH molar concentration in the solution contacting the PVA cryogel was calculated as:

$$[\text{DNPH}] = 25 \times A_{360} / \epsilon_{360} \text{ using } \epsilon_{360} = 15900 \text{ M}^{-1} \text{cm}^{-1} \quad (1)$$

found from the linear calibration graph.

The experiments were made using PVA cryogels produced with and without GA activation, as well as with cryogels with reduced aldehyde groups. The aldehyde group concentration in the cryogels (C<sub>ALD</sub>) was calculated from the difference between DNPH concentrations from the reduced and aldehyde-containing samples: C<sub>ALD</sub> = ([DNPH]<sub>ALD</sub> - [DNPH]<sub>RED</sub>) × V<sub>AM</sub>/V<sub>CR</sub>, where the volume of the adsorption mixture V<sub>AM</sub> = 2.5 × 10<sup>-3</sup> L. The calculations were made for several contact times and averaged, see Results and Discussion.

### 2.3.2. Estimation of cryogels pore volume

Cylindrical or thin cryogels with aldehyde functions reduced according to Section 2.2.1 were transferred to 30% ethanol and then, sequentially, to 50, 75 and 99% ethanol and, finally, to cyclohexane and kept at room temperature overnight. The cryogels immersed in cyclohexane were taken out to air and weighed at times to register the weight loss due to evaporation of the solvent. The dried cryogels were kept for 2 days more at 37 °C to reach the constant weight m<sub>dry</sub>. The obtained data were used to estimate the pore volumes of the gels according to the method [24] and using the equation:

$$V_{\text{pore}} [\text{mL/g}] = (m_{\text{CH}} - m_{\text{dry}}) / d_{\text{CH}} \times m_{\text{dry}} \quad (2)$$

where  $m_{\text{CH}}$  is the weight of the gel immersed in cyclohexane and  $d_{\text{CH}}$  is the density of cyclohexane.

### 2.3.3. Spectrophotometry of thin PVA gel films

The cryogel-coated glass slides produced according to Section 2.2.1 were defrosted in contact with deionized water and rinsed with water. Some of the gels were treated by GA and washed as described in Section 2.2.1. To stain the gels with DNP, these were treated with 1 mM DNP solution in 90% ethanol, containing 40 mM  $\text{H}_2\text{SO}_4$  at room temperature for 24 h, and non-reacted DNP was removed by rinsing with several fresh portions of the same solvent (5 mL) at slow small-angle rocking, until the washings became colorless. The cryogel-coated slides were vertically positioned in a 1 cm-cuvette in 90% ethanol containing 40 mM  $\text{H}_2\text{SO}_4$  and UV-VIS spectra were recorded in the 325–600 nm range for DNP-treated and pristine gels with a wavelength step of 0.5 nm. The spectra of the immobilized DNP were obtained by digital subtraction of the pristine gel spectrum from those of the stained gels. The pristine gel spectrum was an average of three independently made gels.

### 2.3.4. Estimation of trypsin activity in solution

BAPNA trypsin substrate (3.2 mg) was dissolved in 0.3 mL DMSO. The solution (176  $\mu\text{L}$ ) was further diluted by 3.75 mL PBS to produce 1 mM BAPNA solution. The trypsin solution (10 mg/mL) used for the immobilization (Section 2.2.2) was diluted 10-fold by PBS, and 10  $\mu\text{L}$  of the diluted solution (0.01 mg trypsin) was added to 1 mL of 1 mM BAPNA placed into a 1 cm-cuvette. The increasing absorbance of *p*-nitroaniline (*p*-NA) released due to the enzymatic hydrolysis was measured at  $\lambda_{\text{max}} = 410 \text{ nm}$ , the slope of the linear time dependence gave  $A_{410}/\text{min}$ . The activity of trypsin,  $A_0$ , was calculated as

$$A_0 (\text{nmol } p\text{-NA}/\text{min} \times \text{mg trypsin}) = A_{410}/\text{min} \times 10^9 \times 10^{-3} \text{ L} / 8800 \text{ M}^{-1} \text{ cm}^{-1} \times 1 \text{ cm} \times \text{enzyme amount (0.01 mg)} \quad (3)$$

where  $8800 \text{ M}^{-1} \text{ cm}^{-1}$  is the *p*-NA molar extinction coefficient at 410 nm, 1 cm is the optical path and  $10^{-3} \text{ L}$  - solution volume in the cuvette.

### 2.3.5. Estimation of immobilized trypsin activity

1 mM BAPNA solution (140  $\mu\text{L}$ ) was added to the wells containing trypsin immobilized on thin cryogels as well as to the wells with cryogels without enzyme, see Supporting Materials. Absorbance in the wells with cryogel films was registered at 410 nm using a Power Wave XS ELISA reader both before adding the BAPNA solution and during the enzymatic hydrolysis. To calculate the absorbance of the released *p*-NA, the background absorbance of the cryogel films as well as the inherent absorbance of 1 mM BAPNA were subtracted from the  $A_{410}$  values in the corresponding wells. The *p*-NA absorbances from four independent wells were averaged. Activity of trypsin immobilized in the cryogels ( $A_{\text{imm}}$ ) was calculated as

$$A_{\text{imm}} (\text{nmol } p\text{-NA}/\text{min}) = A_{410}/\text{min} \times 10^9 \times 0.18 \times 10^{-3} \text{ L} / 8800 \text{ M}^{-1} \text{ cm}^{-1} \times 0.6 \text{ cm} \quad (4)$$

where  $8800 \text{ M}^{-1} \text{ cm}^{-1}$  is the *p*-NA molar extinction coefficient at 410 nm,  $0.18 \times 10^{-3} \text{ L}$  is the solution volume in the well and 0.6 cm – the optical path.

### 2.3.6. Scanning electron microscopy

Samples for electron microscopy and IR spectroscopy were obtained from the wet monoliths synthesized as described in Section 2.2.1 and cut into round ( $\varnothing 8 \text{ mm}$ ), ca. 2 mm-thick pieces. The pieces were transferred into 30 % ethanol, then, sequentially, into 50, 75 and 99% ethanol and dried in air to constant weight. SEM micrographs were obtained as described in [22] directly from uncoated samples (*i.e.* no sputtering) using a Zeiss EVO LS10 scanning electron microscope equipped with a LaB6 filament. Imaging was done in variable pressure mode at 10 Pa using a backscatter detector, at 20kV accelerating voltage, 250 pA probe current and 6–7 mm working distance.

## 3. Results and Discussion

### 3.1. Pore volume and microscopic appearance of cylindrical and thin PVA cryogels

The PVA cryogel monoliths produced in this study were flow permeable sponges with interconnected macropores typical of similar PVA materials reported earlier [12, 22, 25], see Figure 2a. Thin PVA cryogels were opal translucent films exhibiting a squamous pattern in wet state, visible under microscope, see Figure 2b, with the squama plates arranged at a low angle to the surface and sized from ca.  $50 \times 50 \mu\text{m}$  to  $100 \times 300 \mu\text{m}$ . Apparently, the pattern is an impression of the ice crystals formed as a result of the PVA-GA reaction mixture freezing on the cold glass, see Section 2.2.1. The films could be separated from the glass supports, mechanically transferred with forceps, replaced from one solvent to another, see Figure 2c, dried and weighed. For pore volume estimation, see Section 2.3.2 and Eq. (2), the cryogels were step-wise immersed in ethanol of increasing concentrations and further into cyclohexane. The latter is a non-solvent for PVA, causes no swelling of the gel but instead fills its pores by the volume, which can be calculated from the weight loss during solvent evaporation. Table 1 lists the values of pore volumes obtained for thin and cylindrical cryogels, either additionally treated by GA or not. Kinetic curves of cyclohexane evaporation can be found in Supporting Materials. As follows from the table, the shape and material of the reaction vessel (a syringe or a glass plate) had almost no effect on the pore volume of prepared cryogels. The porosity of thin cryogels was still high and similar to that of cylindrical ones. On the other hand, additional treatment by GA slightly increased the pore volume of cryogels, perhaps by making the pore walls more compact, and this effect was noticeable with both thin and cylindrical samples.

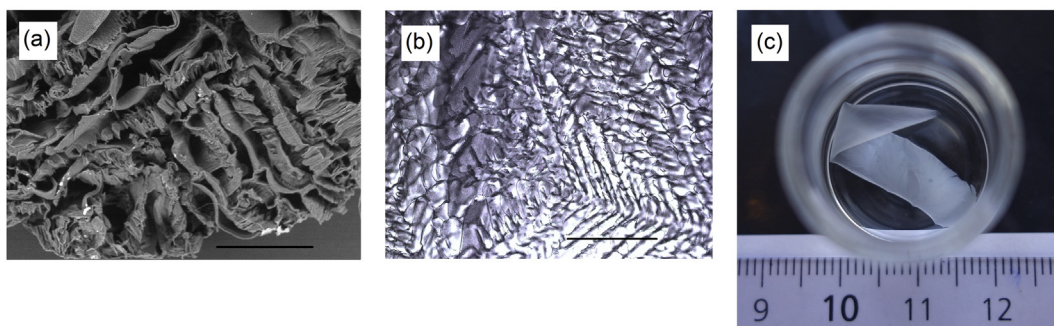


**Figure 2.** (a) SEM image of a cylindrical PVA cryogel cross-section. (b) Light microscopy image of a thin PVA cryogel film on glass surface. (c) Thin PVA cryogel film in 99% ethanol. Scale bars are 500  $\mu\text{m}$ .



**Table 1.** Pore volumes ( $V_{\text{pore}}$ ) of film and cylindrical cryogels additionally treated or non-treated by glutaraldehyde.

Cryogel shape	GA-treated, mL/g dry PVA	Non-treated, mL/g PVA
Film	$9.5 \pm 0.3$	$7.2 \pm 0.3$
Cylindrical	8.5	7.5

Films of PVA cross-linked by GA were earlier proposed [26] and studied [27] as matrices for immobilization of biopolymers. However, pore volume, reactive group content and optical characteristics of these films have not been reported in the cited studies. Transparent PVA films were also used as matrices for embedment of semiconductor nanocrystals [28] and enabled studies of the nanocrystal's absorption spectra. Large pores of thin PVA hydrogels synthesized under semi-frozen state create opportunities for biomolecule immobilization by covalent attachment to the pore walls instead of entrapment in the gel matrix [27]. Significant exposure of the biomolecules to the constituents of the permeant liquid may facilitate biorecognition phenomena such as immune complex formation described in Section 3.4.

### 3.2. Estimation of aldehyde groups in cryogels and spectrophotometry of cryogel films

For estimation of the aldehyde group content, the extensively washed wet monoliths were cut into ca. 2 mm-pieces and combined with ethanolic DNPH solution, see Section 2.3.1. Molarity of DNPH in the reaction mixture was calculated using Eq. (1). Reaction of the surface-bound aldehyde groups with DNPH resulted in decreasing concentration of the reagent in the contacting solution, see Figure 3. The largest uptake of DNPH took place during its contact with PVA-cryogels additionally activated with glutaraldehyde (GA), while the GA concentration chosen for the activation (1%, 2.5% or 10%) did not exert any significant effect on the aldehyde content in the gels (data not shown). Some DNPH binding was also observed with non-activated PVA-cryogels and even with PVA-cryogels treated with sodium borohydride for the reduction of aldehyde groups. In the last case, the quick decrease of the DNPH concentration from 1 mM to ca. 0.8 mM was due to the dilution by water contained in the pores of aldehyde-free cryogel (ca. 0.5 mL gel added to 2

mL of the DNPH solution, see Section 2.2.2). Further slow decrease in DNPH concentration indicated weak adsorptive interaction between the reagent and the polymer. This apparently non-covalent binding of DNPH to polymer gels has not been reported in the literature and needs to be considered when analytical techniques for estimation of aldehydes in powders or porous polymer beads are developed. The content of aldehydes in the activated and non-activated cryogels could, therefore, be calculated as the difference between the total amount of adsorbed DNPH and the amount of DNPH absorbed by the aldehyde-free cryogel. This difference seems to be almost constant at contact times longer than 24 h and thus the contents of aldehydes were calculated using four later pairs of experimental points, see Figure 3, and averaged. The contents of aldehydes were  $0.71 \pm 0.07 \mu\text{mol/mL gel}$  and  $2.4 \pm 0.3 \mu\text{mol/mL gel}$  for the non-activated and GA-activated cryogels, respectively.

The relatively low aldehyde group content may be the result of the mostly bifunctional character of GA cross-linking leaving little free active groups. Nevertheless, the flat 100–130  $\mu\text{m}$ -thick cryogels produced on glass slides were brightly colored by the covalently attached DNPH, see Figure 4, and might be read off spectrophotometrically. It is important to note that cryogels in the reduced form did not show any coloration by DNPH after the washing (Figure 4, line 3). This indicated effective reduction of the aldehydes by sodium borohydride under the chosen conditions. The same figure illustrates the spectra of 50  $\mu\text{M}$  DNPH reagent (line 5) and the reagent combined with 25-molar excess of GA (10  $\mu\text{L}$  25% GA per 1 mL 1mM DNPH, the mixture diluted 20-fold, line 6). As follows from Figure 4, formation of hydrazone via the reaction of DNPH with GA results in relatively small spectral changes, the wavelength of maximum absorbance shifts from 353 nm to 350 nm while the extinction coefficient slightly increases. A similar shift of UV-spectrum to lower wavelengths resulted from hydrazone formation between DNPH and formaldehyde as reported in [29]. In contrast, the UV-spectra of PVA-bound hydrazones showed a red shift and exhibited their maxima at higher wavelengths. This effect seems to be similar to solvatochromism recently reported for various 2,4-dinitrophenylhydrazones in organic solvents and can be ascribed to intramolecular interactions between the

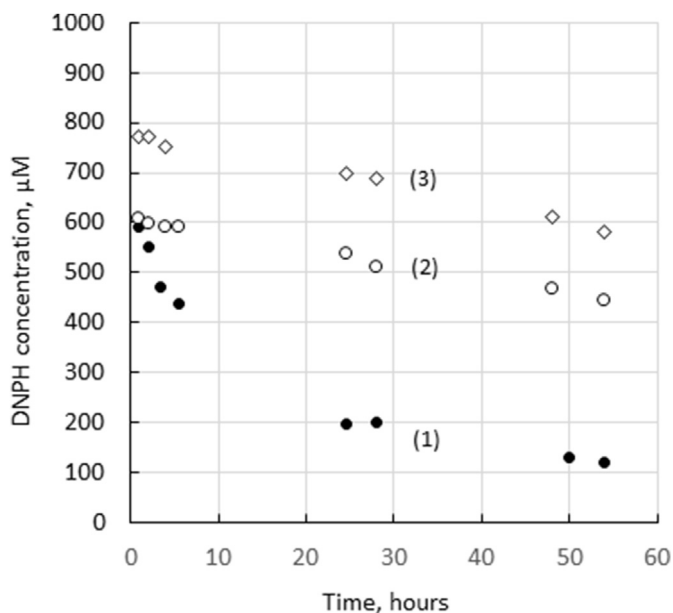


**Figure 3.** DNPH concentration in the solution contacting 2 mm-pieces of PVA-cryogels (total gel volume 0.54 mL) activated with 1% glutaraldehyde (1), non-activated (2), treated with 50 mM  $\text{NaBH}_4$  (3), as a function of time.

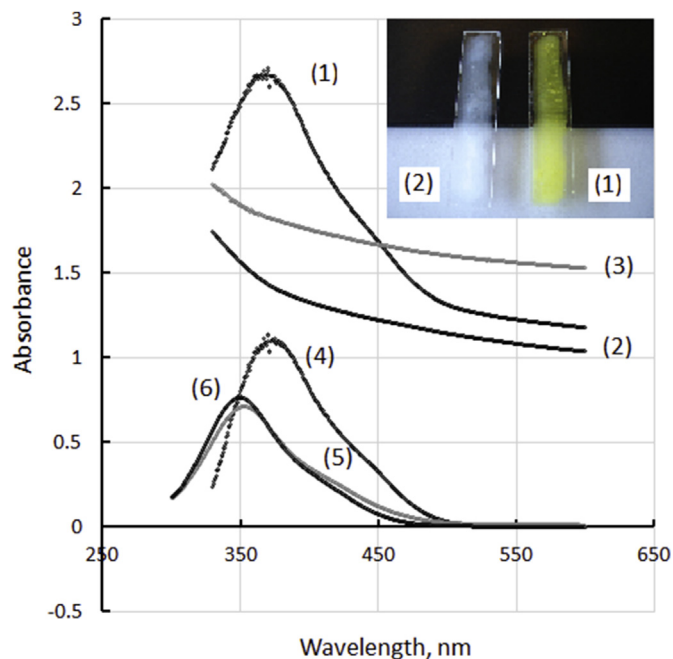


**Figure 4.** UV-VIS spectra of thin PVA cryogels: (1) activated by 1% GA and stained with 50  $\mu\text{M}$  DNPH; (2) average spectrum of three non-activated gels; (3) non-activated gel, reduced by  $\text{NaBH}_4$ ; (4) difference spectrum: (1)–(2); (5) 50  $\mu\text{M}$  DNPH; (6) 50  $\mu\text{M}$  DNPH + 1.25 mM GA. Solvent: 90% ethanol, containing 40 mM  $\text{H}_2\text{SO}_4$ .

PVA segments and the immobilized DNPH as its nitro groups are strong acceptors of hydrogen bond [30].

### 3.3. Enzymatic activity of trypsin immobilized on thin cryogels made in the wells of 96-well plates

To quantify the amount of protein immobilized on GA-activated PVA-cryogels, we have chosen trypsin, a very well-studied enzyme, in combination with its substrate BAPNA that hydrolyses to form the colored product *p*-nitroaniline (*p*-NA). The catalytic activity of free trypsin measured and calculated as described in Section 2.3.4 and Eq. (3) was found to be  $A_0 = 80 \text{ nmol } p\text{-NA}/\text{min} \times \text{mg enzyme}$ . The average activity of immobilized trypsin in cryogels ( $A_{\text{imm}} = 1.1 \text{ nmol } p\text{-NA}/\text{min}$ ) was calculated as described in Section 2.3.5, using Eq. (4), from the slopes of  $A_{410} - A_{410\text{cr}}$  time dependences (1) and (2) illustrated in Figure 5. Two independently synthesized crygel series, each containing eight 40  $\mu\text{L}$ -gel samples were studied. Four of eight gels were used to immobilize the enzyme and to run the catalytic reaction, and the other four were used to evaluate the involvement of non-enzymatic hydrolysis, see Supporting Materials. The standard deviations from the average values of *p*-NA release were moderate, see Figure 4, the enzymatic hydrolysis exhibited similar rates in four independent wells. The background absorbance of PVA cryogels at 410 nm was in the range of 1.8–2.0, which still allowed measurements of the absorbance increasing due to the released *p*-NA because the instrument (see Section 2.3) could measure absorbances up to 4 optical units. The non-enzymatic hydrolysis of BAPNA was negligible, see line 3 in Figure 5. No BAPNA hydrolysis was seen in the empty wells, see Figure 4 of Supporting Materials, indicating no noticeable trypsin adsorption on polystyrene. On the assumption that the enzyme retained its activity after immobilization, one may calculate that  $13.7 \pm 1.3 \mu\text{g}$  enzyme was immobilized per 40  $\mu\text{L}$ -cryogel, which corresponds to 0.34 mg trypsin/mL cryogel. Trypsin typically retains 60–80% of its initial activity after being immobilized on solid supports [31], so the amount of immobilized protein could be somewhat higher than the above given value. The chemical attachment of trypsin was independently confirmed by FTIR-spectroscopy, see Supporting Materials.

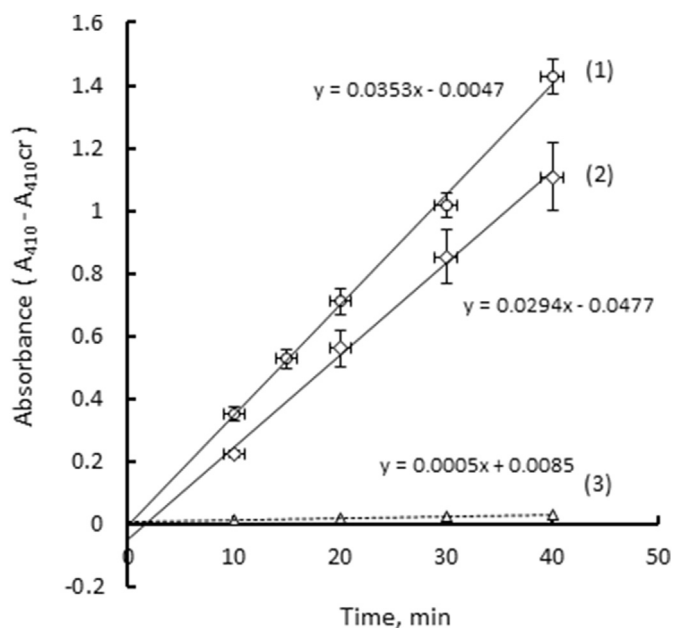


**Figure 5.** *p*-Nitroaniline accumulation in the wells of 96-well plate due to enzymatic hydrolysis of BAPNA. Lines (1) and (2) were obtained with two different preparations of GA-activated thin PVA cryogels. Line (3) corresponds to spontaneous hydrolysis of BAPNA in contact with PVA cryogels without trypsin. Experimental points are averages of 4 independent measurements. The vertical error bars are standard deviations.

Similar amounts of the enzyme laccase (0.57 mg/g wet carrier) were obtained by its immobilization on GA-activated PVA cryogel [15]. Relatively low immobilized amounts of the enzymes are probably a consequence of the low specific surface area of macropores most accessible for the enzymes in PVA cryogels produced via cross-linking by GA. While their  $S_{\text{BET}}$  was estimated as  $78 \text{ m}^2/\text{g}$ , the  $S_{\text{macro}}$  calculated using the modified Nguyen-Do method [32] was only  $2 \text{ m}^2/\text{g}$  [33].

### 3.4. Immobilization of human immunoglobulin G (IgG) and its detection with anti-human peroxidase conjugated rabbit IgG

Human IgG was immobilized at various concentrations on the GA-activated gels situated in the wells of a 96-well plate and combined with anti-human peroxidase conjugated rabbit IgG solution as described in Section 2.2.3. Enzymatic activity of the bound conjugate was estimated with TMB-ELISA substrate solution, by registration of the colored product at 450 nm directly in the wells of the plate. After the background absorbances of the cryogels were subtracted from the registered values, the average differential absorbances ( $A_{450} - A_{450\text{cr}}$ ) were calculated as  $0.31 \pm 0.10$ ,  $0.126 \pm 0.075$ ,  $0.086 \pm 0.020$  and  $0.02 \pm 0.04$  corresponding to  $\gamma$ -globulin concentrations of 10, 1, 0.1 and 0 mg/mL concentrations, respectively, see Figure 6. Catalytic activity of the bound peroxidase conjugate increased with IgG concentration taken for coupling to the PVA-gels, exhibiting the pattern typical of conventional enzyme-linked immunosorbent assay (ELISA). No human IgG adsorption could be registered on the cryogel-free surface of Polystyrene Microtest plates under similar binding (1 M  $\text{NaHCO}_3$ , pH 8.4) and washing conditions. On the other hand, the protein-free cryogels in the neutral reduced form still exhibited non-specific binding of the IgG-peroxidase conjugate. To decrease these effects one needed extensive washing of the gels before adding TMB substrate, see Section 2.2.3. Some of commercial PVA-based porous beads are also known to adsorb immunoglobulins non-specifically, while covalent attachment of hydrophilic amino acids (serine, asparagine) to the beads was shown to diminish the adsorption [34]. In spite of the above limitations, the cryogel-immobilized IgG could certainly be recognized by the anti-human rabbit antibodies in a concentration-dependent manner. This confirmed good permeability of cryogel pores and accessibility of the

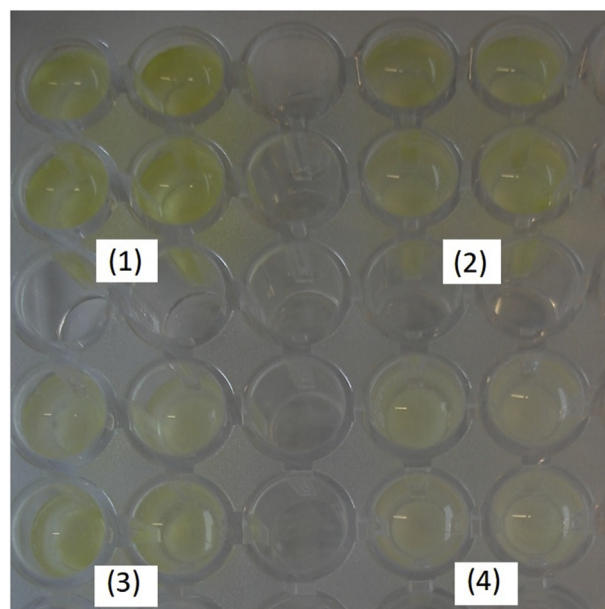


**Figure 6.** Formation of TMB colored product in the wells with specifically adsorbed anti-human peroxidase conjugated rabbit IgG. Concentrations of human IgG taken for immobilization were (1) 10 mg/mL, (2) 1 mg/mL, (3) 0.1 mg/mL, (4) no IgG.

surface-immobilized immunoglobulins for the high-molecular weight (200–240 kDa) protein conjugate.

### 3.5. Related achievements and prospects

The multiwell plate format was earlier employed for accommodating metal-chelating cryogel monoliths aimed at screening of peptide affinity tag libraries. Fluorescence intensity of variously tagged green fluorescence proteins bound to the cryogels via the tags was quantified and the choice of most appropriate tags was made [35]. This approach to design high-throughput biospecific adsorption techniques has got a number of followers [36] including the authors of the present study. Immobilization of specific ligands on the surfaces of flow-permeable translucent cryogels may create opportunities for development of a wide range of analyses, for example, for capture, concentrating and subsequent detection of heavy metal ions and dyes [4, 37, 38] from natural sources. Recently, chitosan hydrogels loaded with the chromogenic substrate of  $\beta$ -glucuronidase, the enzyme secreted by *E. coli* strains, were employed to detect the enzyme in bacterial supernatants [39]. Lateral migration of IgG-conjugated magnetic nanoparticles through porous membranes accompanied by their specific, localized binding to the membrane-coupled antigens could be easily visualized and allowed for antigen identification [40]. The above and many similar applications might be realized using thin macroporous cryogel films described in the present study. Combination of their inherent porosity and translucency with specific binding capacity is a challenging feature calling for development of new environmental and biochemical photometric analytical techniques.

### 4. Conclusions

We have prepared thin, highly porous cryogels of poly(vinyl alcohol) by covalent cross-linking with glutaraldehyde under semi-frozen conditions, carried out on glass slides or in the wells of microtiter plates. The gels were mechanically transferable translucent films with micro squama texture allowing for covalent immobilization of proteins and further reactions with low and high molecular weight biomolecules. The content of reactive aldehyde groups and amounts of protein immobilized in the gels were quantified. Formation of colored substances either bound to or released from the gels could be registered by direct spectrophotometry of the gel films due to their translucency. The results suggest applications of thin reactive PVA hydrogels in photometric analytical techniques using both conventional or microtiter plate formats.

### Declarations

#### Author Contribution Statement

Alexander Ivanov: Conceived and designed the experiments; Performed the experiments; Analyzed and interpreted the data; Wrote the paper.

Lennart Ljunggren: Conceived and designed the experiments; Analyzed and interpreted the data; Contributed reagents, materials, analysis tools or data; Wrote the paper.

#### Funding Statement

This work was supported by Swedish National Public Employment Agency (Arbetsförmedlingen) to enable AEI's collaboration with Vitro-Sorb AB and Malmö University. This work was also supported by Sweden's innovation agency VINNOVA [Ref. 2018–02329].

#### Competing Interest Statement

The authors declare no conflict of interest.

### Additional information

Raw data associated with this study has been deposited at Mendeley under the accession number <https://doi.org/10.17632/2ggs5x8923.1>.

Processed data associated with this study has been deposited at Mendeley under the accession number <https://doi.org/10.17632/6wsdzj5yfm.1>.

Supplementary content related to this article has been published online at <https://doi.org/10.1016/j.heliyon.2019.e02913>.

### Acknowledgements

The authors are thankful to Dr. Tobias Halthur (CR Competence AB, Lund, Sweden) for carrying out the SEM experiments.

### References

- [1] S.V. Mikhailovsky, I.N. Savina, M. Dainiak, A.E. Ivanov, I.Y. Galaev, *Biomaterials/cryogels*, in: Chapter 5.03, second ed., in: M. Moo-Young, M. Butler, C. Webb, A. Moreira, B. Grodzinski, Z.F. Cui, Spiros Agathos (Eds.), *Comprehensive Biotechnology*, 5, Elsevier, 2011, pp. 11–22.
- [2] V.I. Lozinsky, A brief history of polymeric cryogels, *Adv. Polym. Sci.* 263 (2014) 1–48.
- [3] M.M. Eyadeh, M.A. Weston, J. Juhasz, K.R. Diamond, Translucent poly(vinyl alcohol) cryogel dosimeters for simultaneous dose buildup and monitoring during chest wall radiation therapy, *J. Appl. Clin. Med. Phys.* 17 (2016) 308–319.
- [4] E.A. Reshetnyak, N.V. Ivchenko, N.A. Nikitina, Photometric determination of aqueous cobalt (II), nickel (II), copper (II) and iron (III) with 1-nitroso-2-naphthol-3,6-disulfonic acid disodium salt in gelatin films, *Cent. Eur. J. Chem.* 10 (2012) 1817–1823.
- [5] S. Hajizadeh, A.E. Ivanov, M. Jahanshahi, M.H. Sanati, N.V. Zhuravleva, L.I. Mikhailovska, I.Yu. Galaev, Glucose sensors with increased sensitivity based on composite gels containing immobilized boronic acid, *React. Funct. Polym.* 68 (2008) 1625–1634.
- [6] B. Vilozny, A. Schiller, R.A. Wessling, B. Singaram, Multiwell plates loaded with fluorescent hydrogel sensors for measuring pH and glucose concentration, *J. Mater. Chem.* 21 (2011) 7589–7595.
- [7] A. Mateescu, Y. Wang, J. Dostalek, U. Jonas, Thin hydrogel films for optical biosensor applications, *Membranes* 2 (2012) 40–69.
- [8] A.E. Ivanov, V.P. Zubov, Smart polymers as surface modifiers for bioanalytical devices and biomaterials: theory and practice, *Russ. Chem. Rev.* 85 (2016) 565–584.
- [9] V.I. Lozinsky, L.G. Damshkaln, K.O. Bloch, P. Vardi, N.V. Grinberg, T.V. Burova, V.Y. Grinberg, Cryostructuring of polymer systems. XXIX. Preparation and characterization of supermacroporous (spongy) agarose-based cryogels used as three-dimensional scaffolds for culturing insulin-producing cell aggregates, *J. Appl. Polym. Sci.* 108 (2008) 3046–3062.
- [10] I.U. Allan, B.A. Tolhurst, R.V. Shevchenko, M.B. Dainiak, M. Illsley, A. Ivanov, H. Jungvid, I.Y. Galaev, S.L. James, S.V. Mikhailovsky, S.E. James, An in vitro evaluation of fibrinogen and gelatin containing cryogels as dermal regeneration scaffolds, *Biomater. Sci.* 4 (2016) 1007–1014.
- [11] M.G. Drozdova, D.S. Zaytseva-Zotova, R.A. Akasov, A.S. Golunova, A.A. Artyukhova, O.O. Udartseva, E.R. Andreeva, D.E. Lisovyv, M.I. Shtilman, E.A. Markvicheva, Macroporous modified poly(vinyl alcohol) hydrogels with charged groups for tissue engineering: preparation and in vitro evaluation, *Mater. Sci. Eng. C* 75 (2017) 1075–1082.
- [12] F.M. Plieva, M. Karlsson, M.R. Aguilar, D. Gomez, S. Mikhailovsky, I.Yu. Galaev, B. Mattiasson, Pore structure of macroporous monolithic cryogels prepared from poly(vinyl alcohol), *J. Appl. Polym. Sci.* 100 (2006) 1057–1066.
- [13] S. Hajizadeh, H. Kirsebom, A. Leistner, B. Mattiasson, Composite cryogel with immobilized concanavalin A for affinity chromatography of glycoproteins, *J. Sep. Sci.* 35 (2012) 2978–2985.
- [14] A. Kumar, A. Rodriguez-Caballero, F.M. Plieva, I.Yu. Galaev, K.S. Nandakumar, M. Kamihira, R. Holmdahl, A. Orfao, B. Mattiasson, Affinity binding of cells to cryogel adsorbents with immobilized specific ligands: effect of ligand coupling and matrix architecture, *J. Mol. Recognit.* 18 (2005) 84–93.
- [15] M.D. Stanescu, M. Fogorasi, B.L. Shaskolskiy, S. Gavrilas, V.I. Lozinsky, New potential biocatalysts by laccase immobilization in PVA cryogel type carrier, *Appl. Biochem. Biotechnol.* 160 (2010) 1947–1954.
- [16] A.N. Generalova, S.V. Sizova, T.A. Zdobnova, M.M. Zarifullina, M.V. Artemyev, A.V. Baranov, V.A. Oleinikov, V.P. Zubov, S.M. Deyev, Submicron polymer particles containing fluorescent semiconductor nanocrystals CdSe/ZnS for bioassays, *Nanomedicine* 6 (2011) 195–209.
- [17] N.H. Beyer, M.Z. Hansen, C. Schou, P. Højrup, N.H.H. Heegaard, Optimization of antibody immobilization for on-line or off-line immunoaffinity chromatography, *J. Sep. Sci.* 32 (2009) 1592–1604.
- [18] C.F.H. Allen, The identification of carbonyl compounds by use of 2-nitrophenylhydrazine, *J. Am. Chem. Soc.* 52 (1930) 2955–2959.
- [19] S. Uchiyama, M. Ando, S. Aoyagi, Isomerization of aldehyde-2,4-dinitrophenylhydrazone derivatives and validation of high-performance liquid chromatographic analysis, *J. Chromatogr. A* 996 (2003) 95–102.

- [20] B. Gupta, M. Tummalapalli, B.L. Deopura, M.S. Alam, Functionalization of pectin by periodate oxidation, *Carbohydr. Polym.* 98 (2013) 1160–1165.
- [21] S.K. Shannon, G. Barany, Colorimetric monitoring of solid-phase aldehydes using 2,4-dinitrophenylhydrazine, *J. Comb. Chem.* 6 (2004) 165–170.
- [22] A.E. Ivanov, T. Halthur, L. Ljunggren, Flow permeable composites of lignin and poly(vinyl alcohol): towards removal of bisphenol A and erythromycin from water, *J. Environ. Chem. Eng.* 4 (2016) 1432–1441.
- [23] T. Eichorn, A.E. Ivanov, M.B. Dainiak, A. Leistner, I. Linsberger, H. Jungvid, S.V. Mikhailovsky, V. Weber, Macroporous composite cryogels with embedded polystyrene divinylbenzene microparticles: synthesis, characterization and adsorption of toxic metabolites from blood, *J. Chem.* (2013), 348412.
- [24] M.V. Dinu, M.M. Perju, E.S. Drăgan, Porous semi-interpenetrating hydrogel networks based on dextran and polyacrylamide with superfast responsiveness, *Macromol. Chem. Phys.* 212 (2011) 240–251.
- [25] A.E. Ivanov, O.P. Kozynchenko, L.I. Mikhailovska, S.R. Tennison, H. Jungvid, V.M. Gun'ko, S.V. Mikhailovsky, Activated carbons and carbon-containing poly(vinyl alcohol) cryogels: characterization, protein adsorption and possibility of myoglobin clearance, *Phys. Chem. Chem. Phys.* 14 (2012) 16267–16278.
- [26] K.C.S. Figueiredo, T.L.M. Alves, C.P. Borges, Poly(vinyl alcohol) films crosslinked by glutaraldehyde under mild conditions, *J. Appl. Polym. Sci.* 111 (2009) 3074–3080.
- [27] M.A.P. Nunes, P.C.B. Fernandes, M.H.L. Ribeiro, High-affinity water-soluble system for efficient naringinase immobilization in poly(vinyl alcohol)-dimethyl sulfoxide lens-shaped particles, *J. Mol. Recognit.* 25 (2012) 580–594.
- [28] A.I. Savchuk, V.I. Fediv, Ye.O. Kandyba, T.A. Savchuk, I.D. Stolyarchuk, P.I. Nikitin, Platelet-shaped nanoparticles of PbI<sub>2</sub> and PbMnI<sub>2</sub> embedded in polymer matrix, *Mater. Sci. Eng. C* 19 (2002) 59–62.
- [29] M. Tummalapalli, B. Gupta, A UV-Vis spectrophotometric method for the estimation of aldehyde groups in periodate-oxidized polysaccharides using 2,4-dinitrophenyl hydrazine, *J. Carbohydr. Chem.* 34 (2015) 338–348.
- [30] K. Alizadeh, A. Amraie, Electronic absorption spectroscopic behavior and acidity constants of some new dinitrophenylhydrazone derivatives, *Spectrochim. Acta* 147 (2015) 67–72.
- [31] K. Atacan, B. Çakıroğlu, M. Özacar, Improvement of the stability and activity of immobilized trypsin on modified Fe<sub>3</sub>O<sub>4</sub> magnetic nanoparticles for hydrolysis of bovine serum albumin and its application in the bovine milk, *Food Chem.* 212 (2016) 460–468.
- [32] C. Nguyen, D.D. Do, A new method for characterization of porous materials, *Langmuir* 15 (1999) 3608–3615.
- [33] Y. Zheng, V.M. Gun'ko, C.A. Howell, S.R. Sandeman, G.J. Phillips, O.P. Kozynchenko, S.R. Tennison, A.E. Ivanov, S.V. Mikhailovsky, Composites with macroporous poly(vinyl alcohol) cryogels with attached activated carbon microparticles with controlled accessibility of a surface, *ACS Appl. Mater. Interfaces* 4 (2012) 5936–5944.
- [34] H. Yamada, A. Itoh, Y. Hatanaka, M. Tsukiji, K. Takamori, Screening and analysis of adsorbents for Pemphigus autoantibodies, *Ther. Apher. Dial.* 14 (2010) 292–297.
- [35] A. Hanora, F. Bernaudat, F.M. Plieva, M.B. Dainiak, L. Bülow, I.Yu. Galaev, B. Mattiasson, Screening of peptide affinity tags using immobilized metal affinity chromatography in 96-well plate format, *J. Chromatogr. A* 1087 (2005) 38–44.
- [36] S. Reichelt, C. Elnsner, A. Prager, S. Naumov, J. Kuballa, M.R. Buchmeiser, Amino-functionalized monolithic spin-type columns for high-throughput lectin affinity chromatography of glycoproteins, *Analyst* 137 (2012) 2600–2607.
- [37] E.S. Dragan, M.V. Dinu, Progress in polysaccharide/zeolites and polysaccharide hydrogel composite sorbents and their applications in removal of heavy metal ions and dyes, *Curr. Green Chem.* 2 (2015) 342–353.
- [38] H. Ahmad Panahi, M. Abdouss, F. Ghiabi, E. Moniri, A. Mousavi Shoushtari, Modification and characterization of poly(ethylene terephthalate)-grafted-acrylic acid/acryl amide fiber for removal of lead from human plasma and environmental samples, *J. Appl. Polym. Sci.* 124 (2012) 5236–5246.
- [39] M.-M. Sadat Ebrahimi, B. Steinhoff, H. Schönherr, Rapid remote detection of *Escherichia coli* via a reporter-hydrogel coated glass fiber tip, *Eur. Polym. J.* 72 (2015) 180–189.
- [40] A.A. Tregubov, I.L. Sokolov, A.V. Babenyshev, P.I. Nikitin, V.R. Cherkasov, M.P. Nikitin, Magnetic hybrid magnetite/metal organic framework nanoparticles: facile preparation, post-synthetic biofunctionalization and tracking in vivo with magnetic methods, *J. Magn. Magn. Mater.* 449 (2018) 590–596.